

On the Physical Connections between Galaxies of Different Types

Shude Mao and H.J. Mo [★]

Max-Planck-Institut für Astrophysik Karl-Schwarzschild-Strasse 1, 85748 Garching, Germany

Accepted Received; in original form

ABSTRACT

Galaxies can be classified in two broad sequences which are likely to reflect their formation mechanism. The ‘main sequence’, consisting of spirals, irregulars and all dwarf galaxies, is probably produced by gas settling within dark matter haloes. We show that the sizes and surface densities along this sequence are primarily determined by the distributions of the angular momentum and formation time of dark haloes. They are well reproduced by current cosmogonies provided that galaxies form late, at $z \lesssim 2$. In this scenario, dwarf ellipticals were small ‘disks’ at $z \sim 1$ and become ‘ellipticals’ after they fall into cluster environments. The strong clustering of dwarf ellipticals is then a natural by-product of the merging and transformation process. The number of dwarf galaxies predicted in a cluster such as Virgo is in good agreement with the observed number. On the other hand, the ‘giant branch’, consisting of giant ellipticals and bulges, is probably produced by the merging of disk galaxies. Based on the observed phase-space densities of galaxies, we show that the main bodies of *all* giant ellipticals can be produced by dissipationless mergers of high-redshift disks. However, high-redshift disks, although denser than present-day ones, are still not compact enough to produce the high *central* phase space density of some low-luminosity ellipticals. Dissipation must have occurred in the central parts of these galaxies during the merger which formed them.

Key words: galaxies: formation - galaxies: structure - galaxies: ellipticals - cosmology: theory - dark matter

arXiv:astro-ph/9707344v2 4 Aug 1997

1 INTRODUCTION

Galaxies exhibit a wide range in luminosities, sizes and shapes. Their shapes divide them into spirals, ellipticals and irregulars, whereas their sizes and luminosities distinguish giants from dwarfs. Dwarf galaxies (here defined as having a magnitude $\mathcal{M} \gtrsim -16$), while fainter, dominate the observed number counts of galaxies (see Ferguson & Binggeli 1994 for a review). These galaxies can be roughly divided into two morphological classes: dwarf ellipticals (dE's) and dwarf irregulars (dI's). The dI's share many common properties of the more luminous disk galaxies: their profiles are roughly exponential, they are gas rich, rotationally supported and mostly reside in the field. Hence they are generally believed to be the low-luminosity extension of the more luminous late-type galaxies. By comparison, dE's are more puzzling: on the one hand, they show some similar properties to the dI's, for example, their radial profiles are roughly exponential (Faber & Lin 1983), and they follow a similar correlation between the surface brightness and the absolute luminosity (see §2); on the other hand, their isophotes are elliptical, they reside mainly in clusters of galaxies and at least some bright dE's seem to be supported by random motions (Bender & Nieto 1990). These latter properties are reminiscent of giant ellipticals. The question naturally arises whether these dE's are low-luminosity analogues of giant ellipticals or have the same origin as the late-type galaxies. So far three formation scenarios have been proposed. The first suggests that dE's have evolved from dI's (Searle & Zinn 1978; Faber & Lin 1983; Wirth & Gallagher 1983). The second advocates dE's as tidal debris from more massive systems (Gerloa, Carnevali & Salpeter 1983; Hunsberger, Charlton & Zaritsky 1996 and references therein). The third postulates dE's as the end-product of more massive galaxies which have suffered from substantial mass loss (Vader 1986, 1987, and references therein). In this paper, we test the first scenario in the context of hierarchical structure formation models (White & Rees 1978). Specifically, we propose that the main properties of disk galaxies, dI's and dE's are produced by gas settling into the center of dark matter haloes. Hence, dE's are initially small 'disks' [†]; they are transformed into dE's in high density regions like clusters by environmental effects, such as pressure induced star formation (Babul & Rees 1992) and/or galaxy harassment (Moore, Lake & Katz 1997). The strong clustering properties of the dE's are therefore inherently

* E-mail: (smao; hom)@mpa-garching.mpg.de

[†] Note that we use 'disks' to name objects which are roughly rotationally supported; whether or not they are flattened thin disks is not important in our discussion.

related to this transformation process. We study the range of sizes and surface brightnesses expected in such a scenario, using a recent model of galactic disks (Mo, Mao & White 1997, hereafter MMW; see also Dalcanton, Spergel & Summers 1997). We take into account the different star formation efficiency in galaxies using a self-regulated star formation model (White & Frenk 1991). We show that our disk model plus a simple star formation law can reproduce the overall observed properties quite well if the present-day dwarf galaxies form late ($z \lesssim 2$). We also discuss giant ellipticals as the products of merging of disks formed at high redshift. We find that high-redshift disks, although denser, are still not compact enough to produce the high *central* phase space density in some ellipticals, and therefore, dissipation must have played some role in the final formation stage of these inner regions. On the other hand, the main bodies of all ellipticals *can* be produced by dissipationless merging, since their “average” phase space densities are comparable to those of spirals.

The outline of our paper is as follows. In Section 2, we present the observational data to be used. In Section 3, we present our model and compare the model predictions with the observations. In Section 4, we study the connection between disk and elliptical galaxies using phase space density arguments. In Section 5, we discuss some implications and future tests for our model.

2 OBSERVATIONAL DATA

In Figure 1, we show the effective radius, r_{eff} , and the effective surface brightness, $\langle\mu\rangle_{\text{eff}}$, as functions of the B band absolute magnitude, \mathcal{M}_B , for galaxies from different sources. Here r_{eff} is defined as the radius within which half of the light is contained, and $\langle\mu\rangle_{\text{eff}}$ is the mean surface brightness within this radius. For all the samples, we have adjusted the distances and magnitudes to a Hubble constant of $h = 0.5$. The data for dwarf ellipticals (dE’s) from Binggeli & Cameron (1991, 1993) are shown as open circles, with the nucleated ones shown with an additional central dot. Their data were based on a B-band photographic survey of dE’s in the Virgo cluster. The selection function for this sample is given roughly by the long dashed line. The data for normal spirals are from Impey et al. (1996), which also contain many dwarf irregulars (dI’s). These data points are shown as skeletal triangles. We have converted their surface brightness at the effective radius to the effective surface brightness by subtracting 0.7 mag; a correction appropriate for an exponential disk. The selection function for this sample is schematically shown as the short dashed curve. The

data for dwarf spheroidals (dSph) in the local group are adopted from Mateo (1997). This data set (shown as filled squares) is in good agreement with that in Irwin & Hatzidimitriou (1995). We have converted their V band magnitudes using $B - V \approx 0.8$. The effective surface brightness is derived from the central surface brightness by assuming an exponential profile. Fig. 1 also schematically shows the region populated by the ellipticals and galactic bulges from Burstein et al. (1997, hereafter BBFN; see also Bender, Burstein & Faber 1992). To avoid overcrowding, no data points are shown. Note that this large data set includes all types of galaxies. Furthermore it not only lists r_{eff} , $\langle\mu\rangle_{\text{eff}}$, but also gives other kinematic information, such as the central velocity dispersion. This kinematic information will be used to study the phase space density for disk and elliptical galaxies in §4.

As one sees from the figure, the distributions of galaxies in the $\langle\mu\rangle_{\text{eff}}-\mathcal{M}_B$ and $r_{\text{eff}}-\mathcal{M}_B$ planes seem to follow two well-defined sequences. The broad ‘main sequence’ is defined by the spirals, dE’s, dI’s and dSph’s. In this sequence, brighter galaxies have systematically higher effective surface brightness (i.e. lower value of $\langle\mu\rangle_{\text{eff}}$), a trend first noticed by Kormendy (1977, see also Binggeli & Cameron 1991). Note that the sequence is also clearly modulated by the selection effects. The continuation of the trend from dSph’s, dI’s and dE’s to normal spirals, plus the fact that the profiles of these galaxies are fairly good exponentials, is suggestive of a common origin for these classes of objects. For a given absolute magnitude, the range in r_{eff} is about one decade while the scatter in $\langle\mu\rangle_{\text{eff}}$ is about five magnitudes. The question we want to address here is what determines these ranges.

The other sequence, which we term as the ‘Giant branch’, is defined by the giant ellipticals and galactic bulges. Unlike the main sequence, brighter galaxies in the Giant branch have systematically lower surface brightness, and their profiles follow more closely the $r^{1/4}$ -law. These suggest a different formation mechanism from that of the main sequence. The question is then what distinguishes these two sequences and what are their connections.

3 THE MAIN SEQUENCE

3.1 The model

We consider galaxy formation in a cosmological context. For simplicity, we will only consider an Einstein-de Sitter universe, with $\Omega_0 = 1$ and no cosmological constant. The present day Hubble constant is written as $H_0 = 100h \text{ km s}^{-1} \text{ Mpc}^{-1}$, and we take $h = 0.5$. The initial density perturbation power spectrum is taken to be that of the standard cold dark

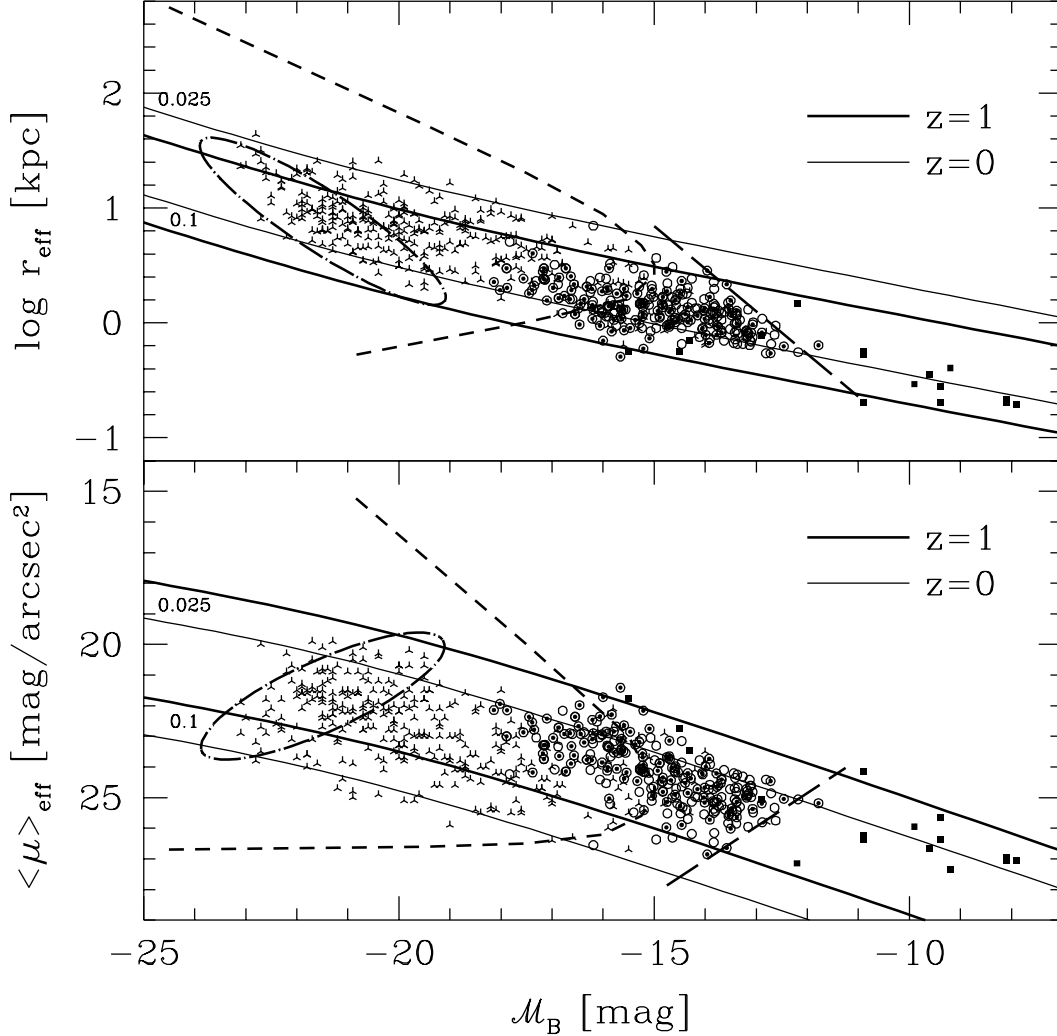


Figure 1. Effective radii, (r_{eff}), and effective surface brightnesses (lower panel), $\langle \mu \rangle_{\text{eff}}$, are shown as a function of the B-band absolute magnitude, \mathcal{M}_B , for different types of galaxies. The spiral and dwarf galaxies from Impey et al. (1996) are shown as the skeletal triangles. The open circles with central dots represent the nucleated dwarf galaxies. The filled squares indicate the dSph's in the local group (Mateo 1997). The short and long thick dashed lines are the selection functions for the Impey et al. sample and the Binggeli and Cameron sample, respectively. The galaxies observed in these samples are to the left of these curves. The region populated by the elliptical galaxies and bulges (Burstein et al. 1997) are indicated by the dot-dashed curves. The thin and thick solid lines are the predicted curves for disk galaxies assembled at the present day and at $z = 1$ in the SCDM model, respectively. For each formation redshift, two curves are shown for two spin parameters, $\lambda = 0.025$ and $\lambda = 0.1$. The predictions for other structure formation models are similar.

matter (SCDM) model with $\sigma_8 = 0.6$. Our results do not change significantly when other cosmogonies are used.

In a recent paper, Mo, Mao & White (1997, hereafter MMW) studied the formation of disk galaxies in the context of hierarchical structure formation (e.g. White & Rees 1978; White & Frenk 1991). The model reproduces the observed properties of disk galaxies rea-

sonably well. Briefly, this model assumes that the gas and dark matter are initially uniformly mixed. Due to dissipative and radiative processes, the gas component adiabatically settles into a disk. Under the assumptions that the resulting mass profile is exponential and that there is no angular momentum loss from the gas to the dark matter, the size and mass profile of a disk can be determined. The initial density profiles of dark haloes are modeled by

$$\rho(r) = \frac{V_h^2}{4\pi Gr^2} \frac{1}{[\ln(1+c) - c/(1+c)]} \frac{r/r_h}{(r/r_h + 1/c)^2}, \quad (1)$$

where

$$V_h^2 = \frac{GM}{r_h}, \quad r_h = \left[\frac{GM}{100H^2(z)} \right]^{1/3}, \quad (2)$$

with M being the mass of the halo, and $H(z) = H_0(1+z)^{3/2}$ the Hubble's constant at the time when the halo is assembled (Navarro, Frenk & White 1996, hereafter NFW). The quantity c in equation (1), called the concentration factor of the halo, can be calculated for a given halo in any given cosmogony (see NFW). The mass of the disk formed in a halo at redshift z is then

$$M_d = m_d M \approx 1.7 \times 10^{11} M_\odot h^{-1} \left(\frac{m_d}{0.05} \right) \left(\frac{V_h}{250 \text{ km s}^{-1}} \right)^3 \left[\frac{H(z)}{H_0} \right]^{-1}, \quad (3)$$

where m_d is the fraction of the total halo mass which settles into the disk. We take $m_d = 0.05$, consistent with the baryon density, $\Omega_{B,0}$, derived from cosmic nucleosynthesis with $h = 0.5$ (Walker et al. 1991). From the (assumed) conservation of angular momentum of a disk during collapse, the disk scale length and surface density are given by (MMW)

$$R_d = \frac{1}{\sqrt{2}} \lambda r_h F_R \approx 8.8 h^{-1} \text{ kpc} \left(\frac{\lambda}{0.05} \right) \left(\frac{V_h}{250 \text{ km s}^{-1}} \right) \left[\frac{H(z)}{H_0} \right]^{-1} F_R, \quad (4)$$

$$\Sigma_0 = \frac{M_d}{2\pi R_d^2} \approx 380 \frac{M_\odot}{\text{pc}^2} h \left(\frac{m_d}{0.05} \right) \left(\frac{\lambda}{0.05} \right)^{-2} \left(\frac{V_h}{250 \text{ km s}^{-1}} \right) \left[\frac{H(z)}{H_0} \right] F_R^{-2}, \quad (5)$$

where λ is the spin parameter of the halo, and the factor F_R takes into account the disk self-gravity and can be approximated as

$$F_R \approx \left(\frac{\lambda}{0.1} \right)^{-0.06+2.71m_d+0.0047/\lambda} (1 - 3m_d + 5.2m_d^2) \frac{1 - 0.019c + 0.00025c^2 + 0.52/c}{[2/3 + (c/21.5)^{0.7}]^{1/2}} \quad (6)$$

(see MMW for details).

Equations (1)-(6) determine the mass distribution in our model. To make a connection to the observed light distribution, we need to specify how efficiently the baryonic gas forms stars. Unfortunately, this process is not well understood; so far only phenomenological descriptions of star formation have been developed. White & Frenk (1991) argued that star formation is self-regulated, and the star formation efficiency in a galaxy is determined by the

balance of supernovae heating and radiative cooling. This model predicts a star formation efficiency that is correlated with halo circular velocity:

$$\epsilon_* = \frac{1}{1 + \epsilon_0(700 \text{ km s}^{-1}/V_h)^2}. \quad (7)$$

For $\Omega_{B,0} = 0.05$, White & Frenk (1991) found that $\epsilon_0 = 0.03$ is compatible with the observed luminosity density in the universe and the mean metallicity of galaxies. This is similar to the value $\epsilon_0 = 0.02$ derived by Dekel & Silk (1986) based on a more elaborate treatment of supernova remnant evolution. We shall take $\epsilon_0 = 0.03$, while cautioning that this parameter is rather uncertain (cf. White & Frenk 1991). To calculate the expected light from the mass that can form stars, we also need to adopt a *stellar* mass-to-light ratio. We assume this mass-to-light ratio to be universal in different galaxies and across the surfaces of disks. This is clearly an oversimplification, since the mass-to-light ratio depends on the detailed star formation and merging histories. However, this is probably sufficient for our purpose since we only concentrate on the general trend of galaxies. We shall take a nominal value of $\Upsilon_B = 2.4h$ derived from dynamical studies of disks (Bottema 1997).

From our assumption that disks have exponential surface brightness profiles, the effective radius and the effective surface density can be obtained as

$$r_{\text{eff}} \approx 1.67R_d, \quad \langle \Sigma \rangle_{\text{eff}} \approx 0.36\Sigma_0. \quad (8)$$

Combining equations (4-8) yields the effective surface brightness

$$\langle \mu \rangle_{\text{eff},B} = 23.1 - 2.5 \log \left(\frac{\Sigma_0}{10^2 M_\odot \text{ pc}^{-2}} \frac{1}{\Upsilon_B} \epsilon_* \right), \quad (9)$$

where the central surface density is expressed in units of $M_\odot \text{ pc}^{-2}$. From equation (3), the absolute magnitude of the galaxy is given by

$$\mathcal{M}_B = -19.5 - 2.5 \log \left(\frac{M_d}{10^{10} M_\odot} \frac{1}{\Upsilon_B} \epsilon_* \right). \quad (10)$$

In Figure 1, we show r_{eff} and $\langle \mu \rangle_{\text{eff}}$ as functions of \mathcal{M}_B predicted for disks at $z = 0$ (thin lines) and $z = 1$ (thick lines). Here z refers to the redshifts at which haloes of the disks are assembled. For each z , the upper and lower curves correspond to $\lambda = 0.1$ and $\lambda = 0.025$, respectively. These two values are approximately the upper and lower 10 percentage points of the λ distribution (see MMW). Thus, the two curves represent roughly the upper and lower limits on r_{eff} [or $\langle \mu \rangle_{\text{eff}}$] for a given formation redshift. It is clear that the observed ranges are well reproduced as a result of the distribution of the spin parameter λ , provided $z \lesssim 2$. This means that the haloes of the galaxies in the main sequence should have been

assembled quite recently. This conclusion for present-day disk galaxies has been reached by MMW and in earlier work (e.g., White & Frenk 1991). As we will show below, such late formation is also required for dwarf galaxies, in order for them not to merge into bigger galaxies.

Before we move on to the next subsection, we examine the metallicity and mass-to-light ratio of galaxies implied by our assumed star formation efficiency. As discussed before, the star formation efficiency (i.e., the value of ϵ_0) is normalized primarily by observations of giant galaxies (White & Frenk 1991). It is therefore interesting to see whether this normalization gives correct results for dwarf galaxies. We estimate the metallicity by the instantaneous recycling approximation:

$$\frac{Z}{Z_\odot} = \frac{y}{Z_\odot} \epsilon_* = \frac{y}{Z_\odot} \frac{1}{1 + \epsilon_0 (700 \text{ km s}^{-1} / V_h)^2}, \quad (11)$$

where $y \sim Z_\odot$ is the metal yield of stars (Binney & Tremaine 1987, p. 565). We adopt $y = 1.2Z_\odot$ as suggested by White & Frenk (1991). The predicted line is shown in Figure 2, together with the data points for nearby dSph's (Irwin & Hatzidimitriou 1995). Notice that the predicted line has a scaling of $Z \propto L^{2/5}$, since $L_B \propto M_d \epsilon_* \propto V_h^5$ and $Z \propto V_h^2$. This trend is clearly in agreement with the observations. The predicted amplitude also agrees with the observational results within a factor of two. Irwin & Hatzidimitriou (1995) and Mateo (1997) also derive the “total” mass-to-light ratio for dSph's, based on the assumption that mass follows light. This assumption is clearly violated in our model, since dark matter dominates in the outer part. A direct comparison is thus problematic. We approximately identify their “total” mass-to-light ratio as that within the effective radius. The total mass within the effective radius is $M_d/2 + M_h(< r_{\text{eff}})$, and the total light is $(M_d/2) \times \epsilon_* / \Upsilon_B$. The mass-to-light ratio is therefore given by

$$\frac{M}{L_B} = \Upsilon_B \left(1 + \frac{M_h(< r_{\text{eff}})}{M_d} \right) \frac{1}{1 + \epsilon_0 (700 \text{ km s}^{-1} / V_h)^2}. \quad (12)$$

The prediction of this model is shown in the lower panel of Figure 2, where we have taken the dark matter mass within r_{eff} to equal to the disk mass. As one can see the predicted trend of $M/L_B \propto L_B^{-2/5}$ is in good agreement with the observations. The amplitude is somewhat too high, but this discrepancy should not be taken too seriously since, as discussed above, the comparison between theory and observations is not straightforward. In general, the self-regulated star formation law seems to predict the right trend for dwarf galaxies.

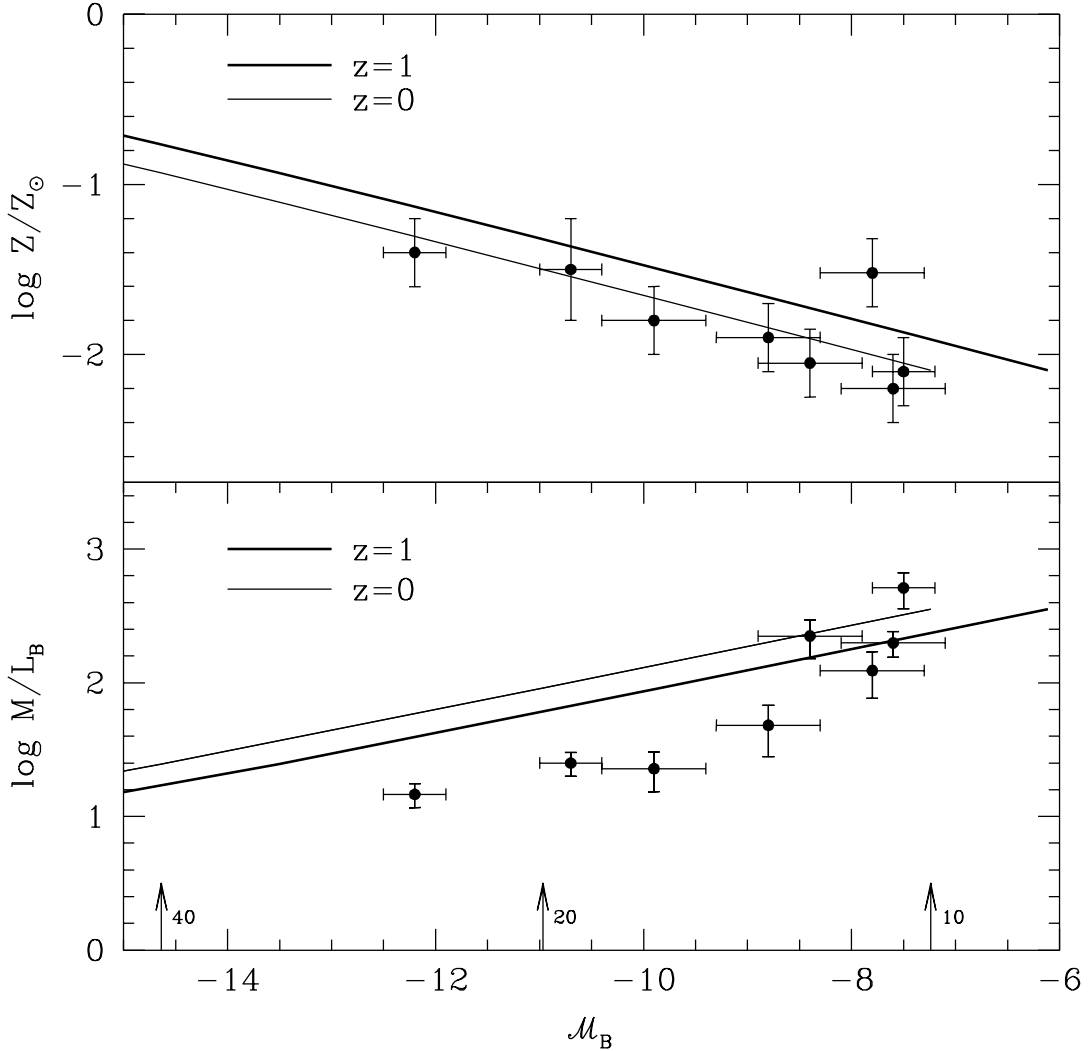


Figure 2. Metallicity (upper panel) and mass-to-light ratio (lower panel) are shown as a function of \mathcal{M}_B for dSph’s in the local group. The thin and thick lines are the model predictions (cf. equations [11 and [12]) for disks assembled at $z = 0$ and $z = 1$, respectively. The three arrows label the magnitudes of disks with circular velocity of 10, 20, and 40 km s^{-1} at $z = 0$, respectively.

3.2 Connections between galaxies of different types

As shown above, spirals, dI’s, dE’s and dSph’s follow the same well-defined sequence in the $r_{\text{eff}} - \mathcal{M}_B$ and $\langle \mu \rangle_{\text{eff}} - \mathcal{M}_B$ planes. The general trend is well reproduced by our simple disk model. In this model, all these classes of objects start out as ‘disks’ forming at $z \lesssim 2$. The disks that remain in the field will manifest themselves as dwarf spirals and dI’s. We propose that those that have already merged into larger haloes such as clusters are transformed into dwarf ellipticals at the present time (see next subsection). There are many processes that

can perform this transformation, such as gas stripping by cluster potential (Faber & Lin 1983) and galaxy harassment (Moore, Lake & Katz 1997). In the transformation process, some gas may also be compressed and flow into the center, forming nucleated dwarf ellipticals (cf. Babul & Rees 1992). Since we link dE's directly with the cluster environment, they should show strong clustering, while dI's should have the same (weak) clustering as the field spirals. Such spatial segregations of dwarf galaxies are indeed observed (cf. Ferguson & Binggeli 1994). Unfortunately, the transformation processes are difficult to quantify. However, recent Hubble Space Telescope (HST) observations give strong support to this picture. These observations revealed that clusters at $z \sim 0.4$ contain a large number of blue late-type galaxies that have disappeared from clusters at the present time (Dressler et al. 1994). These blue galaxies may just be the dwarf 'disks' formed at $z \sim 1$ which are falling into clusters as they are observed. Since in our model dwarf galaxies start out as rotation-supported objects, we expect late-type dwarf galaxies, such as dI's and dwarf spirals, to be supported by their angular momentum. dE's, on the other hand, may have lost some angular momentum in the transformation process and may no longer be rotationally supported. As shown by the simulations of Moore et al. (1997), the interaction between a dwarf spiral galaxy and cluster environment can indeed reduce the rotation substantially, whereas the change in its effective surface density is only modest (less than a factor of order 2). At the moment, there are only a few dwarf elliptical galaxies with kinematic data. The results for some low-luminosity ellipticals suggest that bright dE's are not supported by rotation (Bender & Nieto 1990; see also Peterson & Caldwell 1993). This is contrasted with late-type dwarf galaxies, such as dwarf spirals and dI's, which are clearly supported by rotation (e.g. Salpeter & Hoffman 1996). While the latter observational results are consistent with our model prediction, a much larger kinematic sample is required to explore the kinematic properties of dwarf galaxies.

3.3 The number and formation time of dE's in Virgo type clusters

In the model discussed above, dE's are 'disks' that have merged into larger haloes at the present time. In this section we show that this assumption leads to specific predictions for the number density and formation time of dwarf elliptical galaxies in clusters such as Virgo. These predictions should be compared with observations, taking account of the late formation of these galaxies discussed in §3.1.

In a hierarchical clustering scenario, such as the Λ CDM model considered here, initial density perturbations are amplified by gravitational instability, giving rise to bound clumps (dark haloes) which grow more and more massive as they merge together and accrete surrounding material. Simple analytic models for such hierarchical merging have been developed (Bond et al. 1991; Bower 1991; Kauffmann & White 1993; Lacy & Cole 1993). Using such models, one can calculate the merging history of a dark halo. As a small halo merges into a larger one, its dark matter mixes with that of the larger one to form a new halo. However, if a galaxy (called a satellite galaxy) has already formed at its centre before the merger, this satellite galaxy may retain its identity until it merges with other galaxies in the new halo. The time scale for a satellite to merge depends on its mass relative to that of the halo in which it is orbiting, and can be approximated by a simple law,

$$t_{\text{mrg}} \approx \frac{1}{\ln \Lambda} \left(\frac{r_i}{r_h} \right)^2 \left(\frac{M_{\text{halo}}}{M_{\text{sat}}} \right) \frac{r_h}{V_h}, \quad (13)$$

where M_{sat} is the initial mass of the satellite halo, M_{halo} is the mass of the halo in which the satellite is orbiting, r_i is the initial orbital radius, and $\ln \Lambda \approx 10$ is the Coulomb logarithm (see Binney & Tremaine 1987, §7.1). We assume $r_i = r_h/2$ to roughly take account of possible non-circular orbits.

Given the merging history of a cluster and the time-scale of galaxy merging in dark matter haloes, one can in principle calculate the number of satellite galaxies (cluster members) in the cluster, and the times when the haloes of these galaxies are assembled. Such a treatment of galaxy formation in dark haloes has been developed extensively (e.g. White & Rees 1978; White & Frenk 1991; Kauffmann, White & Guiderdoni 1993; Cole et al. 1994). In this paper, instead of making detailed merging trees, we define a characteristic formation time for a (primary) halo of mass M (identified at cosmic time t), $t_{1/2}$, which is the time when the mass of its largest progenitor reaches $M/2$. If $t - t_{1/2} > t_{\text{mrg}}$, where t_{mrg} is the merging time scale (see equation [13]) for the satellite galaxy under consideration, then the number of such satellite galaxies is given by the number of dwarf progenitor haloes (with masses in the range relevant to dwarf galaxies) at time $t - t_{\text{mrg}}$. This number can be easily obtained from an extension of the Press-Schechter formalism (Press & Schechter 1974, hereafter PS), as discussed in Bower (1991) and Bond et al. (1991). In this case, dwarf galaxies that fall into the cluster earlier are destroyed by galaxy merging, and the effective formation time of the haloes of the remaining dwarf galaxies is just $t - t_{\text{mrg}}$. On the other hand, if $t - t_{1/2} < t_{\text{mrg}}$, dwarf galaxies formed at time $t_{1/2}$ will not be destroyed by subsequent merging of galaxies.

In this case, the number of satellite galaxies is the sum of the number of dwarf progenitor haloes at time $t_{1/2}$ and the number of dwarf galaxies contained in larger progenitors at $t_{1/2}$. The number of dwarf progenitor haloes can, as before, be obtained from the extended PS formalism, while the number of dwarf galaxies contained in larger progenitors can be calculated by repeating the same procedure as for the primary halo. As a result, the total number of dwarf galaxies in the primary halo can be obtained. The formation time of the halo of each dwarf galaxy can also be identified.

In Figure 3, the solid curve shows the predicted numbers of dwarf galaxies as a function of halo circular velocity, V_h . Here dwarf galaxies are defined to be those with B -band luminosities $10^7 L_\odot < L_B < 10^9 L_\odot$, to match the observed ranges of L_B for dE's (Ferguson & Sandage 1991). This luminosity range is transformed into a mass range of dark haloes, as described in §3.1. The observed numbers of dwarf galaxies (mainly dE's) in this luminosity range in the Virgo cluster (with a circular velocity about 800 km s^{-1}) is about 800 (e.g. Ferguson & Sandage 1991). This number for small clusters like Leo and Dorado (with $V_h \sim 250 \text{ km s}^{-1}$) is about 20. As one can see, the predictions are generally in agreement with observations. Similar results have been obtained by Kauffmann et al. (1993) for the dwarfs in the local group and for the brighter galaxies ($\mathcal{M}_B < -15$) in the Virgo cluster. The two dashed curves show the upper and lower quartiles of the formation redshifts of the haloes of dwarf galaxies. It is clear that most dwarf galaxies form rather late, at $z \lesssim 2$, consistent with the late formation required by the observed distributions of r_{eff} and $\langle \mu \rangle_{\text{eff}}$ (see §3.1). The late formation of dwarf galaxies, which is consistent with their observed intermediate age population of stars (e.g. Held & Mould 1994), is somewhat contrary to the intuition that smaller galaxies should form earlier in hierarchical clustering. As is clear in our model, the late formation is due to the fact that small galaxies that form early have merged into larger galaxies.

4 CONNECTION TO GIANT ELLIPTICALS

Toomre & Toomre (1972, see also Toomre 1977) proposed that mostly stellar disks are the building blocks from which more massive early-type galaxies are produced. However, as noted by Carlberg (1986; see also Hernquist et al. 1993), the central phase-space density in elliptical galaxies cannot be achieved by merging of the present-day stellar disks, since the central phase space density in disks is lower and merging cannot increase the (coarse-grained)

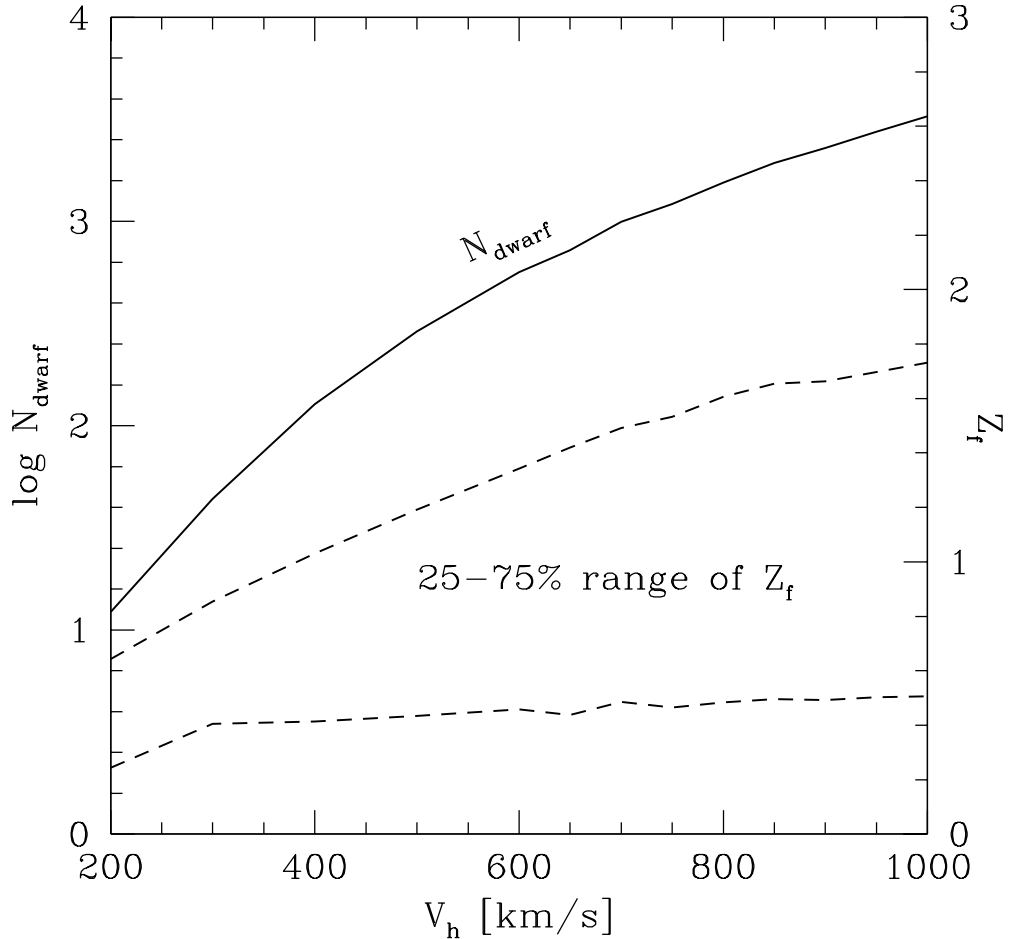


Figure 3. The solid curve shows the number of dwarf galaxies (defined in the text) in haloes as a function of halo circular velocities. The two dashed curves show the upper and lower quartiles of the formation redshifts of dwarf galaxies.

phase space density. However, there remains two important caveats in this argument. First, as shown in MMW, in hierarchical clustering models, disks formed at high redshifts are smaller and denser than present-day disks. Since they also form preferentially in high density regions and hence are more likely to merge to form more massive galaxies, it is important to examine if these high redshift disks are dense enough to be the progenitors of present-day elliptical galaxies. Second, as pointed out by Hernquist et al. (1993), the maximum phase-space density of an elliptical may be associated only with a small fraction of the mass at the centre of the galaxy and so be irrelevant to the main body of the galaxy. An important remaining question is therefore whether or not the main bodies of elliptical galaxies can

still be produced by stellar mergers, even though their central parts cannot. A careful study of the phase space density of galaxies requires detailed knowledges about stellar density distribution and kinematics. Unfortunately, these (particularly the kinematics) are not well known observationally, therefore the calculations are only approximate. Nevertheless, as we shall see below, the conclusions we reach are fairly robust even with the uncertainties involved.

We first consider the central phase space density of disk and elliptical galaxies. The central phase space density can be estimated by dividing the central mass density by the volume occupied by an ellipsoid with its axes equal to the three velocity dispersions. For ellipticals, we adopt the same assumptions as in Carlberg (1986): the density profile of an elliptical is a deprojected Hubble law and the central velocity dispersion is isothermal and isotropic. The central phase space density is then

$$f_c = \frac{27}{16\pi^2} \frac{1}{G} \frac{1}{\sigma_c r_c^2} = \frac{39.5}{\sigma_c r_c^2} \frac{M_\odot}{\text{pc}^3 (\text{km s}^{-1})^3}, \quad (14)$$

where σ_c is the central velocity dispersion in km s^{-1} , and r_c is the radius (in units of pc) at which the surface brightness drops to half of the central value. For disk galaxies, the surface mass density is radially exponential, and we model while the vertical structure as an isothermal sheet with a constant scale height across the disk. The central velocity dispersion in the vertical direction is then given by (e.g., Binney and Tremaine 1987, p. 282)

$$\sigma_{z,0}^2 = 2\pi G \rho_0 z_0^2, \quad \rho_0 = \frac{\Sigma_0}{2z_0}, \quad z_0 = \mathfrak{R}_z R_d, \quad (15)$$

where ρ_0 is the central mass density, and z_0 is the vertical scale height, assumed to be proportional to the disk scalelength by a constant factor \mathfrak{R}_z . We take $\mathfrak{R}_z \approx 0.2$ (Bottema 1997). The vertical velocity dispersion at radius r can be obtained in the same way by simply evaluating ρ and Σ at radius r . We assume that the other two velocity dispersions are proportional to σ_z :

$$\sigma_\theta = \mathfrak{R}_\theta \sigma_z, \quad \sigma_r = \mathfrak{R}_r \sigma_z. \quad (16)$$

The central phase space density of a disk can now be obtained

$$f_c = \frac{\rho_0}{4\pi \sigma_{z,0} \sigma_\theta \sigma_r / 3} = \frac{\Sigma_0}{2R_d} \frac{1}{(\pi G \Sigma_0 R_d)^{3/2}} \frac{3}{4\pi \mathfrak{R}_z^{5/2} \mathfrak{R}_\theta \mathfrak{R}_r}. \quad (17)$$

We shall take $\mathfrak{R}_\theta = \sqrt{2}$, $\mathfrak{R}_r = 2$. These values are motivated by observations of our local disk and the flat rotation curves of disk galaxies (cf. Carlberg 1986). Substituting eqs. (4) and (5) into equation (17) gives

$$f_c = 1880h \frac{M_\odot}{\text{pc}^3 (\text{km s}^{-1})^3} \frac{1}{M_d} \frac{H(z)}{H_0} \times \left(\frac{\lambda}{0.05} \right)^{-3/2} \left(\frac{m_d}{0.05} \right)^{1/2} F_R^{-3/2}. \quad (18)$$

Notice that for a given disk mass, the central phase space density increases with redshift as $H(z)/H_0 = (1+z)^{3/2}$.

Although the central phase space density is valuable for describing the inner region of a galaxy, it does not provide any direct information for the “global” phase space density in a galaxy. We therefore need a measure of the average phase space density of galaxies. Here we define such a quantity as the mass density within the effective radius divided by the volume (in the velocity space) occupied by an ellipsoid with its axes equal to the three velocity dispersions. For disk galaxies, the mass density within the effective radius is $\approx \langle \Sigma \rangle_{\text{eff}} / (2z_0)$, and the velocity volume is $\approx 4\pi\sigma_z\sigma_r\sigma_\theta/3$, therefore the effective phase space density can be estimated as:

$$f_{\text{eff}} \approx \frac{\langle \Sigma \rangle_{\text{eff}}}{2z_0} \frac{1}{4\pi\sigma_z\sigma_r\sigma_\theta/3}, \quad (19)$$

where all the velocity dispersions are evaluated at the effective radius, r_{eff} . Notice that the effective phase space density is actually *higher* than the central value because the velocity volume drops faster than the surface density (cf. Carlberg 1986). Similarly, one can evaluate the effective phase space density for ellipticals, which yields the following expression (Hernquist et al. 1993):

$$f_{\text{eff}} \approx \frac{15\sqrt{3}}{128\pi^2} \frac{1}{G} \frac{1}{\sigma_c r_{\text{eff}}^2}. \quad (20)$$

Equations (19) and (20) are both approximate and are accurate only within a factor of a few.

In the top panel of Figure 4, the data points show the effective phase space densities for the observed disks (open circles) and elliptical galaxies (filled circles) in BBFN. For ellipticals, f_{eff} can be obtained straightforwardly using equation (20), since both σ_c and r_{eff} are given. For the spirals, we first obtain the effective surface density by using $\langle \Sigma \rangle_{\text{eff}} = \langle \mu \rangle_{\text{eff}} / (\Upsilon_{B\epsilon_*})$, then derive the velocity dispersions with equations (15) and (16), and finally calculate f_{eff} from equation (19). The curves in the same panel show the predicted phase-space densities of disks as a function of the B band magnitude and of the redshift z when disk material is assembled. The theoretical predictions nicely bracket the observed disk galaxies. The effective phase space densities of spirals are higher than those of the ellipticals because the stars are concentrated in a much smaller volume (i.e. in a thin plane) and because the velocity dispersions are smaller for disks than those for the ellipticals. Numerical

simulations show that when two comparable stellar disks merge, the coarse-grained phase space density drops by a large factor (Barnes 1992) and the merger remnant resembles an elliptical galaxy. To estimate the remnant effective phase space density, we assume that the circular motion of the initial disk galaxy is converted into random motions while the effective radius remains roughly the same, as suggested by numerical simulations of disk merging (Barnes 1992; Weil & Hernquist 1996). Equation (20) is then appropriate for evaluating f_{eff} for the merger remnant. The results are shown as open squares. They overlap with the data points for ellipticals, indicating that the main bodies of ellipticals can be readily produced by dissipationless mergers of disk galaxies. If ellipticals are formed by repeated merging, Hernquist et al. (1993) argued that for repeated merging of equal mass systems, the phase space density scales as $\propto M^{-2} \propto L_B^{-2}$. This scaling is shown as the heavy dashed line. It reproduces the trend reasonably well, and lends further support to the formation of ellipticals by the merging of disk galaxies. It remains to be seen whether the merging scenario can reproduce the amplitude and scatter in the observed $r_{\text{eff}}\text{-}\mathcal{M}$ relation, and more generally the fundamental plane.

The symbols in the lower panel of Figure 4 show the observed central phase space densities for disks (open circles) and elliptical galaxies (filled symbols). The data for elliptical galaxies are taken from the Faber et al. (1997) HST sample. This sample is ideal because it is designed to study the centres of elliptical galaxies with the excellent HST resolution. Even with the excellent resolution of HST, many ellipticals fainter than -22 magnitude do not show resolved cores at the HST resolution, $0''.1$. For these ellipticals, the half-light radii are estimated by assuming that the central surface brightness is equal to that at $0''.1$. The core radii derived in this way are obviously upper limits and the resulting f_c lower limits. These are shown as filled triangles, in contrast with the resolved ellipticals shown as filled dots. The data for spirals are again from BBFN. f_c is estimated using analogous steps to that for f_{eff} (see last paragraph). This procedure gives the central phase space densities for exponential disks and therefore does not take into account the contribution from bulges, which may have higher central phase space densities. Despite these uncertainties, it seems clear that the central phase space density for ellipticals fainter than -22 magnitude are some three orders of magnitude higher than the observed disks. For giant ellipticals with $\mathcal{M}_B \lesssim -22$ the difference is smaller, about a factor of ten.

The solid curves show the predicted central phase space densities for disks at $z = 0$ and 1, with $\lambda = 0.025$ and 0.1. As before, the model predicts the right range of f_c for disk

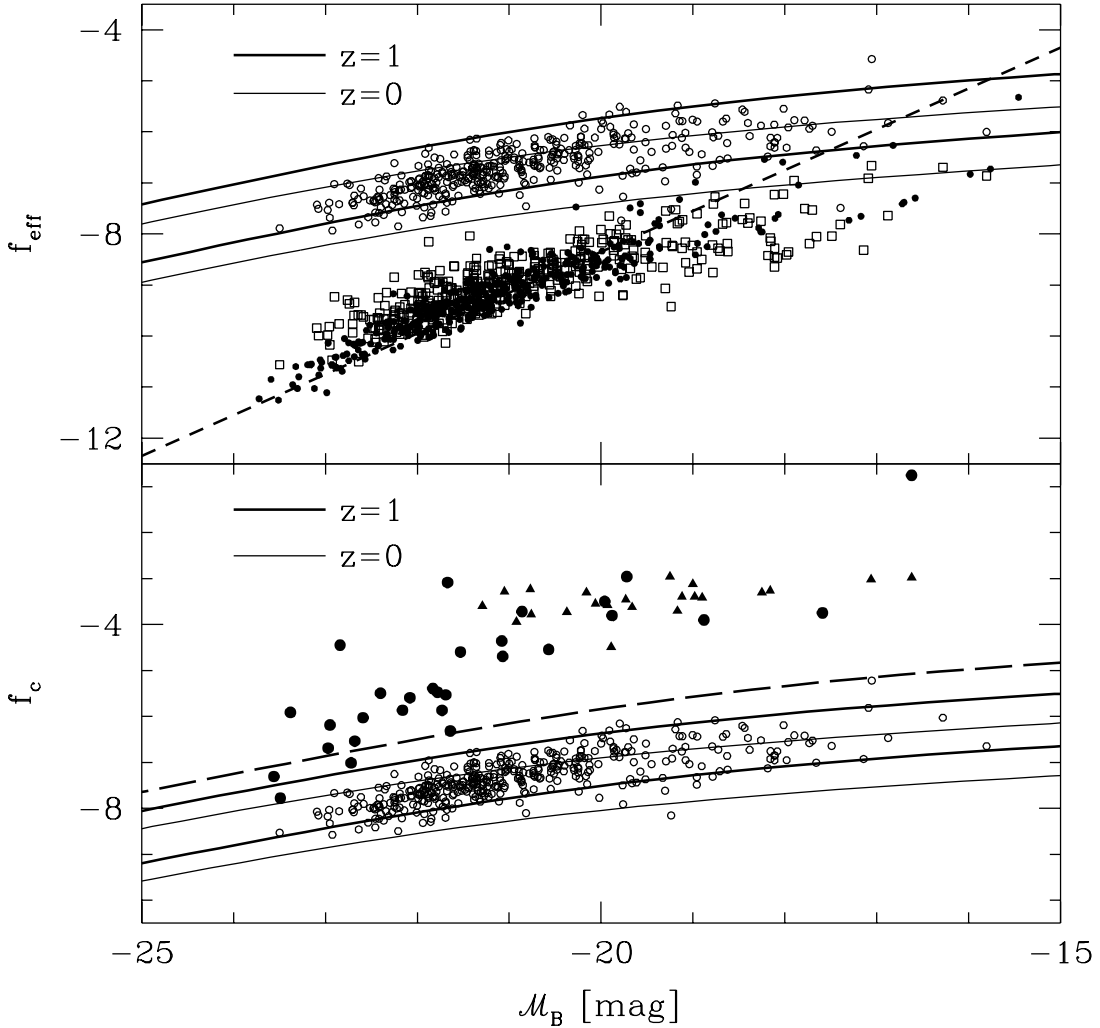


Figure 4. The effective (top panel) and central (lower panel) phase space densities are shown versus the B-band absolute magnitude. All the galaxies are from Burstein et al. (1997) except the HST sample of Faber et al. (1997). The latter sample is used to compute the central phase space density of ellipticals. The open circles in the top panel indicate the effective phase space density estimated with equation (19) whereas the open squares indicate those estimated with equation (20). The latter estimates lie on top of those for ellipticals (shown as filled circles). The thick dashed line indicates the slope predicted for the simplest equal-mass merging (Hernquist et al. 1993). In the lower panel, the filled circles indicate the central phase space density for the core-resolved ellipticals whereas the filled triangles indicate the lower limits for those unresolved ellipticals. The open symbols are again for disk galaxies. The thick and thin solid lines are the predicted curves for disk galaxies assembled at $z = 1$ and $z = 0$ in the SCDM model, respectively. For each formation redshift, two curves are shown for two spin parameters, $\lambda = 0.025$ and $\lambda = 0.1$. The $\lambda = 0.025$ curve is always above the $\lambda = 0.1$ curve. For the central phase space density, we have indicated one additional line for $z = 3$ and $\lambda = 0.025$ (thick long dashed). The range predicted for other structure formation models is similar to the one shown here.

galaxies. In addition, the long dashed curve shows f_c for disks at $z = 3$ with $\lambda = 0.025$. As one can see, although the central phase space densities are higher for disks at high redshifts, the increase is too small to match the observed f_c for the low-luminosity ellipticals. Thus, the central parts of elliptical galaxies, particularly those fainter than $\gtrsim -22$ magnitude,

cannot be formed by dissipationless merging of pure stellar disks. For brighter ellipticals, it is less clear whether dissipation is necessary, since their central phase space densities are comparable to those of fainter disks. Therefore the central parts of the brighter ellipticals can be produced either by dissipation or by small disks (at high redshift) that have merged and settled into the centres of these ellipticals.

5 DISCUSSION

We have examined the connections between galaxies of different types and the two sequences that they seem to follow: the “main sequence” followed by the disk galaxies, dI’s and dE’s, and the “giant sequence” followed by the elliptical galaxies. For the ‘main sequence’, we show that angular momentum has played a crucial role in determining the size and surface brightness of galaxies. For a given circular velocity, the size of objects scales as $\lambda(1+z)^{-3/2}$, while the surface density of object scales $\lambda^{-2}(1+z)^{-3/2}$ (cf. equations [4-5]). For reasonable ranges of spin parameter $\lambda = 0.025 - 0.1$ and formation redshift $z = 0$ to 1, these simple scalings predict a range of size and surface brightness of about one decade and 4.2 magnitudes, in good agreement with the observations. These predicted ranges are nearly independent of detailed model parameters, such as cosmological parameters and mass-to-light ratios. We found that the sequence followed by elliptical galaxies and galactic bulges can be produced by the merging of disk galaxies. The main bodies of ellipticals can be formed by dissipationless merging while some dissipation must have occurred in the central parts of some low-luminosity ellipticals. This conclusion is based on a comparison of the central and the “average” phase space densities of disk and elliptical galaxies.

The role that the angular momentum plays in disk galaxies and dI’s is self-evident since these systems are flattened and are clearly influenced by rotation. However, for the dE’s the evidence for rotational support is weak. In fact, a few bright dE’s are known to be supported by random motions (Bender & Nieto 1990). Unfortunately, the sample so far is very small and is only limited to bright dwarfs, it remains a possibility that the fainter systems are influenced by rotation. Even for the bright dwarfs, the velocity profiles are only measured in the central region (with radius $\lesssim 0.5r_{\text{eff}}$), while in our scenario, most angular momentum is outside this region (for an exponential disk, half of the angular momentum is outside $2.5r_{\text{eff}}$). It will be very interesting to extend the observational sample to fainter dwarfs and also to the outer parts of galaxies. In this picture, dE’s are initially small disk systems, which are later

transformed into dE's, by processes such as galaxy harassment (Moore et al. 1997) or tidal stripping (Faber & Lin 1983) when they enter clusters. The predicted number of dE's that have merged into and survived in clusters is in good agreement with the observed numbers in clusters such as Virgo. This conversion process is directly supported by the HST observation of clusters at $z \sim 0.4$ (Dressler et al. 1994), which found that bulgeless disks dominate the number counts at the faint end. These galaxies have apparently been transformed into dE's since these galaxies dominate nearby clusters such as Virgo and Coma.

ACKNOWLEDGMENTS

We are grateful to Ralf Bender, Yipeng Jing, Roberto Saglia, David Syer, and particularly Simon White for helpful discussions. We also thank Ralf Bender for providing us with data prior to publication. This project is partly supported by the ‘‘Sonderforschungsbereich 375-95 f ur Astro-Teilchenphysik’’ der Deutschen Forschungsgemeinschaft.

REFERENCES

- Babul A., Rees M. J., 1992, MNRAS, 255, 346
 Barnes J. E., 1992, ApJ, 393, 484
 Bender R., Burstein D., Faber, S. M., 1992, ApJ, 399, 462
 Bender R., Nieto J.-L., 1990, A&A, 239, 97
 Binggeli B., Cameron L. M., 1991, A&A, 252, 27
 Binggeli B., Cameron L. M., 1993, A&AS, 98, 297
 Binney J., Tremaine S., 1987, Galactic Dynamics. Princeton Univ. Press, Princeton, NJ
 Bond J. R., Kaiser N., Cole S., Efstathiou G. 1991, ApJ, 379, 440
 Bottema R., 1997, preprint (astro-ph/9706230)
 Bower R. G., 1991, MNRAS, 248, 332
 Burstein D., Bender R., Faber S.M., Nolthenius R., 1997, preprint (astro-ph/9707037) (BBFN)
 Carlberg R. C., 1986, ApJ, 310, 593
 Cole S., Arag on-Salamanca A., Frenk C.S., Navarro J.F., Zepf S.E., 1994, MNRAS, 271, 781
 Dalcanton J.J. Spergel D.N., Summers F.J., 1997, ApJ, 482, 659
 Dekel A., Silk J., 1986, ApJ, 303, 39
 Dressler A., Oemler A., Butcher H., Gunn J.E., 1994, ApJ, 430, 107
 Faber S. M., Lin D. N. C., 1983, ApJ, 266, L17
 Faber S. M., Tremaine S., Ajhar E. A., Byun Y.-I., Dressler A., Gebhardt K., Grillmair C., Kormendy J., Lauer T.D., Richstone D., 1997, preprint (astro-ph/9610055)
 Ferguson H. C., Sandage A., 1991, AJ, 101, 765
 Ferguson H. C., Binggeli B., 1994, A&A review, 6, 67
 Gerola H., Carnevali P., Salpeter E. E. 1983, ApJ, 268, L75
 Held E.V., Mould J.R., 1994, AJ, 107, 1307
 Hernquist L., Spergel D.N., Heyl J.S., 1993, ApJ, 416, 415

- Hunsberger S.D., Charlton J.C., Zaritsky D., 1996, ApJ, 462, 50
- Impey C. D., Sprayberry D., Irwin M.J., Bothun G.D., 1996, ApJS, 105, 209
- Irwin M., Hatzidimitriou D., 1995, MNRAS, 277, 1354.
- Kauffmann G., White S. D. M., 1993, MNRAS, 261, 921
- Kauffmann G., White S.D.M., Guiderdoni B., 1993, MNRAS, 264, 201
- Kormendy J. 1977, ApJ, 218, 333
- Lacey C., Cole S., 1993, MNRAS, 262, 627
- Mateo M. 1997, preprint (astro-ph/9701158)
- Mo H.J., Mao S., White S.D.M. 1997, preprint (astro-ph/9707093)
- Moore B., Lake G., Katz N. 1997, preprint (astro-ph/9701211)
- Navarro J.F. Frenk C.S., White S.D.M., 1996, ApJ, 462, 563 (NFW)
- Navarro J.F., White S.D.M., 1994, MNRAS, 267, 401
- Peterson R.C., Caldwell N., 1993, AJ, 105, 1411
- Press W.H., Schechter P., 1974, ApJ, 187, 425 (PS)
- Salpeter E.E., Hoffmann G.L. 1996, ApJ, 465, 595
- Searle L., Zinn R., 1978, ApJ, 225, 357
- Toomre A., Toomre J. 1972, ApJ, 178, 623
- Toomre A. 1977, in *The Evolution of Galaxies and Stellar Populations*, ed. B.M. Tinsley & R.B. Larson, 401. New Haven: Yale University Observatory
- Vader J.P. 1986, ApJ, 305, 669
- Vader J.P. 1987, ApJ, 317, 128
- Walker T.P., Steigman G., Schramm D. N., Olive K. A., Kang H.-S. 1991, ApJ 376, 51
- Weil M. L., Hernquist L., 1996, ApJ, 460, 101
- White S.D.M., Frenk C.S., 1991, ApJ, 379, 52
- White S.D.M., Rees M.J., 1978, MNRAS, 183, 341
- Wirth A., Gallagher K.S., III, 1983, ApJ, 282, 85

This paper has been produced using the Royal Astronomical Society/Blackwell Science L^AT_EX style file.